

Simulation of Earthquake Ground Motions in the Eastern U.S. Using Deterministic Physics-based and Stochastic Approaches

Sanaz Rezaeian

Research Structural Engineer, U.S. Geological Survey (USGS), Golden, CO, USA

Stephen Hartzell

Geophysicist, U.S. Geological Survey (USGS), Golden, CO, USA

Xiaodan Sun

Associate Professor, Southwest Jiaotong University, Chengdu, China

Carlos Mendoza

Geophysicist, Fugro Consultants Inc., Lakewood, CO, USA

ABSTRACT: Earthquake ground motion recordings are scarce in the central and eastern U.S. (CEUS) for large magnitude events and at close distances. We use two different simulation approaches, a deterministic physics-based model and a stochastic model, to simulate recordings from the 2011 Mineral, Virginia, M_w 5.8 earthquake in the CEUS. We then use the 2001 Bhuj, India, M_w 7.6 earthquake as a tectonic analog for a large CEUS earthquake and modify our simulations to develop models for generation of large magnitude earthquakes in the CEUS. Both models show a good fit to the observations from 0.1 to 10 Hz, and show a faster fall-off with distances beyond 500 km for the acceleration spectra compared to ground motion prediction models (GMPEs) for a M_w 7.6 event.

1. INTRODUCTION

Simulated earthquake ground motions are important in engineering applications, especially in the stable continental regions of the CEUS, where there is a shortage of recorded motions. Simulations can be used in response history analysis or in development of ground motion prediction equations (GMPEs) for use in response spectrum analysis. In this paper, we use two different simulation approaches to develop models that can generate ground motion time-series for moderate to large magnitude events in the eastern U.S.

In the CEUS, recordings from moderate to large magnitude earthquakes (moment magnitudes M_w greater than about 5.5) at close distances that can cause significant damage to structural systems are very rare. Although there are no recordings in the CEUS for a large magnitude event, there is evidence of such earthquakes in the region. For example, the

1811-1812 New Madrid seismic sequence was estimated to have three events with M_w ranging from 6.8 to 8.0 (Petersen et al., 2014). Furthermore, in the 2014 update of the National Seismic Hazard Maps (Petersen et al., 2014), the U.S. Geological Survey (USGS) assumed a magnitude range of 4.7 to 8.0, with varying probabilities of occurrences, to model earthquakes in the CEUS.

Due to lack of recordings, simulations have been utilized for years to develop GMPEs for this region. But most of these simulations are based on simplified approaches such as point-source stochastic modeling and are suitable only for prediction of elastic response spectra. Furthermore, model parameters and assumptions are based on observed data from small magnitude events in the CEUS or the active tectonic regions in the western U.S. (WUS) where ground motion recordings are abundant. As a result, there is large uncertainty in model assumptions and unknown parameters.

Although using WUS data as a guide to identify CEUS parameters might be a helpful approach in the absence of CEUS recordings, ground motion characteristics in the CEUS can be fundamentally different from those in the WUS. The CEUS region has unique tectonic and geologic settings, where relatively thin layers of younger and softer sediments overlay very hard rock, allowing seismic waves to propagate to great distances with lower attenuation than in the WUS (Petersen et al., 2014).

In this paper, we use recordings from two recent earthquakes in stable continental regions in order to simulate the full ground motion waveform for a large magnitude event in the CEUS. For a review of existing simulations, see Sun et al. (2014).

The first event we use is the 2011 M_w 5.8 Mineral, Virginia, earthquake, a moderate magnitude event that is one of the largest instrumentally recorded earthquakes in the CEUS. In Sun et al. (2014), we simulated recordings from this earthquake at 40 broadband stations located 23 to 596 km from the epicenter, using three different simulation approaches. These simulations were used to develop models for generation of ground motions for an event with a similar magnitude at any given distance in the region (see Section 2).

The second event we use is the 2001 M_w 7.6 Bhuj, India, earthquake, a large magnitude event that occurred in the “stable” Indian shield (Singh et al., 2003), which is a tectonic setting more similar to the CEUS than that of the WUS. Regrettably, most on-scale recordings from this earthquake are more than 200 km from the epicenter. We use the Bhuj event as a tectonic analog for a large CEUS earthquake, and apply two different models to simulate recordings from this earthquake at 7 stations with distances from 281 to 1,001 km from the epicenter (Section 3).

In the text that follows, the three simulation models for the Mineral earthquake developed in Sun et al. (2014) are summarized. Next, recorded motions from the Bhuj earthquake are simulated, using a source-based deterministic physics-based

model and a site-based stochastic model. To simulate a larger magnitude earthquake in the CEUS region, we use the Mineral simulations to establish our regional models; then, we extrapolate the parameters of these models to a larger magnitude event using the results of our simulations for Bhuj. The extrapolation to a larger magnitude than the Mineral earthquake and to shorter distances than the Bhuj earthquake is done differently for each of the two simulation models and is described in Section 4. Finally, we compare the elastic response spectra from our simulations for a M_w 7.6 event in the CEUS to existing GMPEs in the region.

2. SIMULATIONS FOR MINERAL EARTHQUAKE M_w 5.8

In Sun et al. (2014), we used three different models to simulate recordings from the Mineral earthquake: (1) a deterministic physics-based simulation model by Hartzell et al. (2005), (2) a source-based stochastic simulation model based on the model of Boore (2003), and (3) a site-based stochastic simulation model by Rezaeian and Der Kiureghian (2010). Comparisons were then made between these three independent simulation approaches, which had not been done directly in the past. In general, physics-based models are known to produce realistic waveforms at long spectral periods (>1 s), but they are computationally intensive and require thorough knowledge of the seismic environment for their source and material models. Stochastic models, on the other hand, may be less accurate in representing the character of actual ground motion recordings, but are computationally tractable and incorporate what is known about ground motion source, path, and site characteristics into simple functional forms. Source-based stochastic models are known to perform best at short spectral periods (<1 s); site-based stochastic models, however, can perform well for a broad range of periods with certain modifications.

We calibrated and modified all three simulation approaches to fit the Mineral data. Modeling details and fitted parameters are

provided in Sun et al. (2014) for each simulation method and are summarized below.

2.1. Deterministic Physics-based Simulation

Deterministic physics-based simulation models are source-based, which means they explicitly describe the fault rupture process at the source, the propagation of the resulting seismic waves, and the effects of local site conditions to generate a time-series at a specific site. These models use a kinematic or dynamic rupture model to define the source, a material model such as a seismic velocity model to define the propagation path, and then solve the wave propagation equation by analytic 1D or numerical 3D models.

To simulate the Mineral earthquake, we used the method of Hartzell et al. (2005), which has the advantage of producing realistic waveforms for a broad range of spectral periods compared to some other physics-based approaches. The source is described by a kinematic rupture model. The source parameters were determined for Mineral by minimizing the Fourier spectra bias using observed motions. For the material model, we used the velocity model of Saikia (1994), which utilizes a laminated flat-layered waveguide with an alternating high- and low-velocity distribution across the crust and upper mantle. We used the Q model of Hartzell and Mendoza (2011) to describe the anelastic attenuation. Finally, because this method subdivides the fault plane into many ‘subfaults,’ the response of each subevent is calculated by summing theoretical Green’s functions for a given velocity model for all frequencies, after which the simulations are corrected for near-surface soil effects using a nonlinear soil correction method (i.e., DESRA2); this model produces realistic synthetic waveforms and provides satisfactory overall bias with respect to the Mineral recordings from 0.1 to 10 s spectral periods (Sun et al., 2014).

2.2. Source-based Stochastic Simulation

We also used a source-based stochastic model based on the method of Boore (2003) to simulate Mineral recordings as a reference. This kind of

simulation is simple and is often used in development of GMPEs, where only the elastic response spectra at short periods is of interest. We modified the method to obtain a better fit to data. But this method assumes stationarity of the frequency content, underestimates the variability, and can only produce one component of ground motion (Sun et al., 2014). This model gives larger bias at long periods (>2 s) than the other two models and is not used in this paper to simulate Bhuj.

2.3. Site-based Stochastic Simulation

The third simulation model, by Rezaeian and Der Kiureghian (2010), is a site-based stochastic model, which uses a stochastic process to describe the ground motion time-series as it is observed at a site; it implicitly accounts for the effects of source, path and site conditions through the model parameters. The stochastic process has six parameters that are fit to recorded motions with known earthquake and site characteristics. Arias intensity, I_a , duration, D_{5-95} , and time at the middle of strong shaking, t_{mid} , control the evolving intensity of the motion; predominant frequency, ω_{mid} , its rate of change with time, ω' , and bandwidth parameter, ζ , control the frequency content of the motion. Probability distributions for the model parameters were identified empirically using the Mineral recordings. Then, regression was used to develop predictive relations for each parameter in terms of distance and site conditions (see Sun et al., 2014).

With this model, one can randomize the parameters based on their distributions, given a distance and site condition, to predict ground motions for a future earthquake of similar magnitude to Mineral. The ease in generating multiple realizations and randomizing the parameters also allows accurate estimation of the variability and better performance when looking at the spatial distribution of residuals. Sun et al. (2014) show that this model provides realistic synthetic waveforms and a satisfactory bias for most periods (0.1 to 10 s), but performs superiorly for periods less than about 1 s.

2.4. Results

Comparisons of the three models to observed motions revealed that all three methods can provide acceptable estimations of response and Fourier spectra for periods less than 2 s. Figure 1 shows the acceleration response spectrum at 0.2 s versus distance for recorded data and for the three simulation methods. For reference, this figure also shows a weighted combination of GMPE medians in the CEUS, according to the USGS model by Petersen et al. (2014). All three simulations show a fall-off with distance similar to the recorded data and to the GMPE. The physics-based and site-based stochastic models show comparable spectral amplitudes, while the source-based stochastic model shows systematically lower amplitudes and a smaller variation.

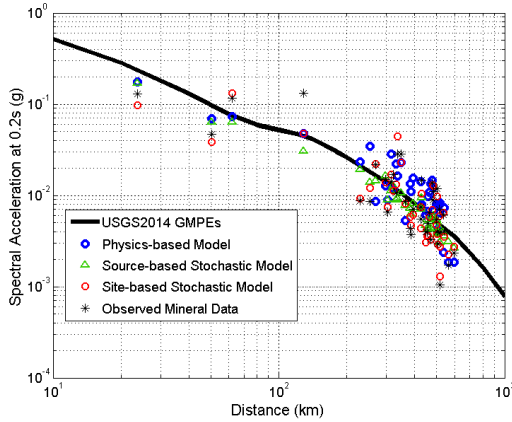


Figure 1: Acceleration response spectrum at 0.2 s for the Mineral recordings, three simulation models, and the 2014 USGS combination of GMPE medians.

Similar figures for other periods are shown in Sun et al. (2014), where the models were also validated in terms of the full waveform and spatial distribution of residuals. In general, the physics-based model performs better at longer periods (>2 s); however, the accuracy of this model is very sensitive to the selection of an appropriate crustal velocity model. The stochastic site-based model works best at shorter periods and allows for easy generation of multiple realizations.

3. SIMULATIONS FOR BHUJ EARTHQUAKE M_w 7.6

In this section, we use the physics-based approach of Hartzell et al. (2005) and the site-based stochastic model of Rezaeian and Der Kiureghian (2010) to simulate the two horizontal components of ground motion recordings from 7 stations located within about 1,000 km of the epicenter of the Bhuj earthquake. These stations and their corresponding distances are listed in Table 1. Note that there are only two recordings available within the 600 km distance range, where we simulated records from the Mineral earthquake.

Table 1: Stations used in Bhuj simulations.

Station Code	Latitude ($^{\circ}$ N)	Longitude ($^{\circ}$ W)	Distance (km)
DGA	23.977	72.75	281
BOM	18.900	72.817	571
PUN	18.53	73.849	663
BHP	23.241	77.4245	740
KAR	17.308	74.183	796
NDI	28.683	77.217	915
JBP	23.167	79.983	1001

The two horizontal components of the ground motion recorded at station BOM and one realization of synthetics for each simulation method are shown in Figure 2 as an example. Details of the simulations are summarized below.

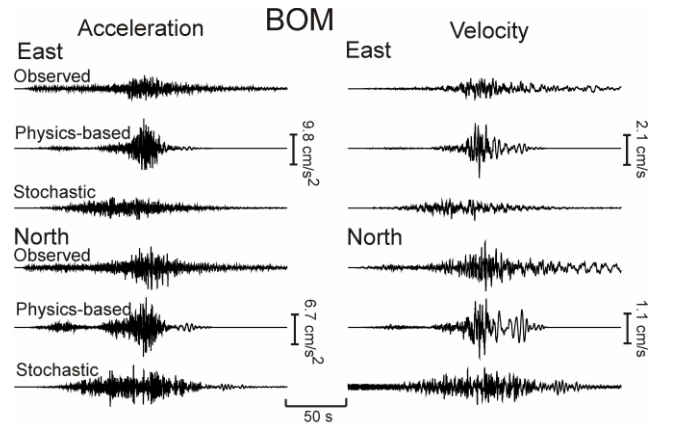


Figure 2: BOM recorded and simulated motions.

3.1. Deterministic Physics-based Simulation

For this earthquake, the source dimensions, mechanism, and other source properties are taken from Antolik and Dreger (2003). Teleseismic inversion suggests a thrust fault with a dip angle of about 50° , and allows us to assume a 50×20.3 km rectangular area, with a hypocenter depth of 16 km and the top of rupture at 9 km below the surface. The Q model was taken from Singh et al. (2003) and is specific to the stable Indian shield. The velocity model, however, is similar to what was used for Mineral due to lack of a regional velocity model for India and the similarity of the tectonic setting to that of the eastern U.S. This velocity model, shown in Sun et al. (2014), allows for random fluctuation of velocities within its many thin velocity layers and was found to successfully generate the regional L_g waves that significantly influence ground motions at large distances.

Two horizontal components of the velocity time-series are generated for each of the seven stations and compared to the recorded motions. Recall that, in this simulation approach, the model parameters are selected to match the Fourier spectra ($f_{0smallest}=2.85$ Hz, $\gamma=2.85$ Hz, $V_R=2.0$ km/s, $h=2.47$ km, $M_{0smallest} = 1.42 \times 10^{24}$ dyne-cm; for description of parameters, see Sun et al., 2014). The bias (solid), standard deviation (dotted), and misfit (dashed), as defined in Sun et al. (2014), for spectral values are shown in Figure 3.

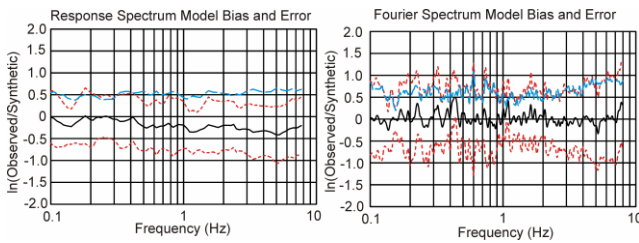


Figure 3: Bias of physics-based simulations for Bhuj.

3.2. Site-based Stochastic Simulation

The model by Rezaeian and Der Kiureghian (2010), described in Section 2.3, is used for stochastic simulations. For each of the recordings in Table 1, we identify the 6 model parameters.

Distribution of these parameters for Bhuj are shown in Figure 4 and are compared to the parameters for Mineral. Due to scarcity of data points, we do not split the time-series into two separate groups of orthogonal components as was done for Mineral, but rather use both components in identification of parameters. Figure 5 shows the bias compared to recordings from Bhuj for acceleration response spectra.

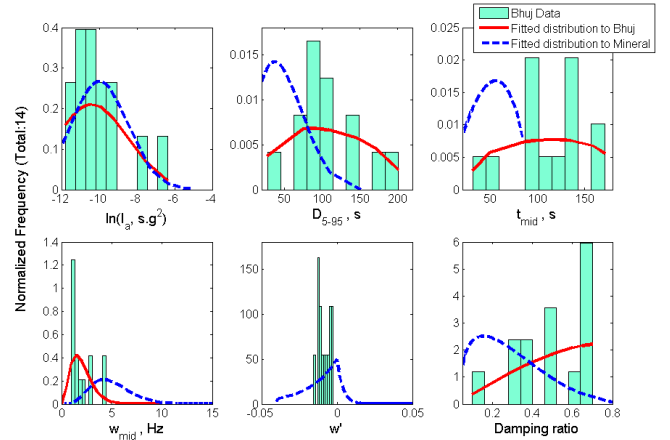


Figure 4: Stochastic model parameters for Bhuj compared to Mineral.

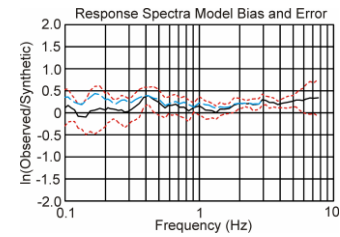


Figure 5: Bias of stochastic simulations for Bhuj.

For simulation of future earthquakes with similar magnitudes to Bhuj, we want to randomize the model parameters and develop predictive equations for each parameter through regression on distance. Using the data in Figure 4, we assign a lognormal distribution to I_a , Beta distributions to D_{5-95} , t_{mid} , and ζ , and a Gamma distribution to ω_{mid} . The rate of change of frequency, ω' , is fixed at -0.008 . Our predictive equations (not shown here) are only in terms of the distance; for Mineral, these equations also included site conditions, which are poorly known in the case of Bhuj recordings.

4. EXTRAPOLATION: SIMULATIONS FOR A M_w 7.6 EVENT IN THE CEUS

In this section, we use our models for simulation of the M_w 5.8 Mineral earthquake in the CEUS and modify them using our simulations from the M_w 7.6 Bhuj earthquake in order to simulate ground motions for a large magnitude earthquake in the CEUS. The extrapolation to a larger magnitude than the Mineral earthquake and to smaller distances than the Bhuj earthquake is done differently for each of the two simulation models, as described below.

4.1. Deterministic Physics-based Simulation

For simulation of a M_w 7.6 event in the CEUS, we use the same source model as derived for the Bhuj earthquake. However, we consider several different fault models that have different fault areas, rupture velocities (V_R), and depths of faulting (D) that are within the uncertainties for these parameters for a CEUS earthquake. Fault dimensions of 40×20 km and 50×20 km are considered, which correspond to stress drops of 300 and 200 bars, respectively. Two different V_R values are tried, 2.0 and 2.7 km/s. Although the lower value was obtained from modeling the Bhuj records, this value may have been forced artificially low by the inversion to fit the long record durations. In addition, hypocenters at a depth of $D=16$ and 10 km are considered. The shallower depth may be more appropriate for CEUS seismicity. The same crustal velocity model is used as in the modeling of the Mineral earthquake with the anelastic attenuation (Q) model of Atkinson (2004).

Using the above assumptions, ground motions were simulated on a 50 km grid around the epicenter of the Mineral earthquake up to a distance of 600 km. Figure 6a shows one realization of the physics-based simulations for $D=10$ km and $V_R=2.7$ km/s. Note that the rupture runs in the northeast-southwest direction.

Several of the source parameters are randomized and many of the localized irregularities in this figure are due to the use of just one sample realization of these parameters. Randomness in the model comes from several

sources: (1) the distribution of fractal subevents; this method is based on subdividing the fault plane into a fractal size distribution of subfaults and a different distribution is used for each realization; and (2) randomizing the normally distributed values of rake, rise time, and rupture time. If many realizations are generated and averaged, we expect to see a smoother spatial pattern, reflecting primarily the radiation pattern and directivity of the source as is shown in Figure 6b for an average of 10 realizations.

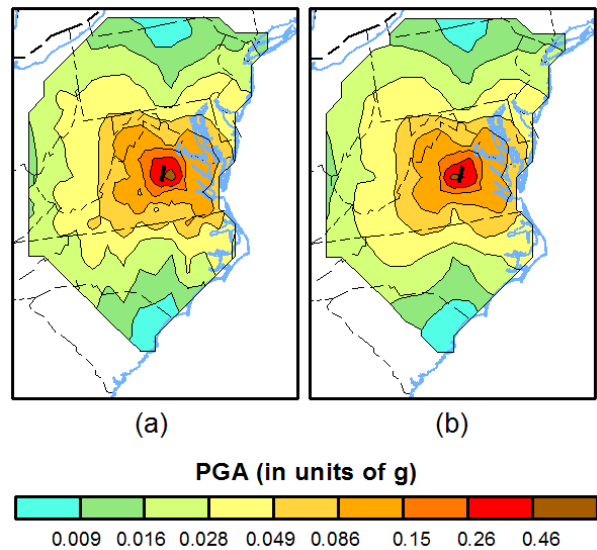


Figure 6: Peak ground acceleration (PGA) for (a) one realization, and (b) average of 10 realizations, of simulations for a M_w 7.6 event.

4.2. Site-based Stochastic Simulation

To develop a model for simulation of ground motions for an earthquake in the CEUS with a magnitude larger than 5.8 using the stochastic model, we use our model parameters from the Mineral simulations.

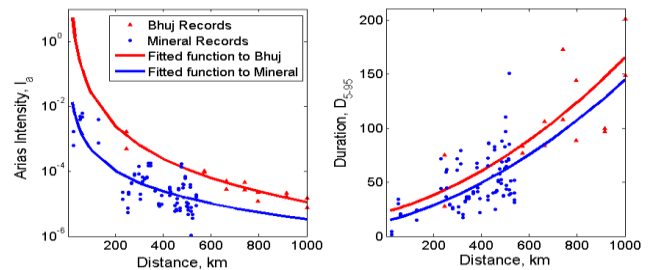


Figure 7: Arias intensity and duration for Mineral and Bhuj. Fitted functions are superimposed.

Recall that each parameter is a function of distance. We then scale them with magnitude using our predicted parameters from the Bhuj simulations. See Figure 7 for parameters I_a and D_{5-95} , where there is a clear scaling pattern with increasing magnitude.

The magnitude scaling model for each of our six parameters is developed in two different ways: (1) we use the Bhuj and Mineral data to develop magnitude scaling models, S_1 , for the distance range of 200 to 600 km, where data from both events are available; then, we extrapolate each model to shorter distances; (2) for the distance range of 200 to 600 km, we follow the above approach, but for distances below 200 km, we use our WUS model from Rezaeian and Der Kiureghian (2010) to develop magnitude scaling models, S_2 . The distance-dependent predictive relations for each model parameter is given below, where P_i represents a model parameter, as listed in Section 2.3. $\Phi^{-1}[F(\cdot)]$ shows transformation to the standard normal space using the distribution of each parameter, R is distance in km, and σ is the standard deviation.

$$\Phi^{-1}[F_{P_i}(p_i)] = \begin{cases} \beta_0 + \beta_1 \ln\left(\frac{R}{705}\right) + \sigma & i = 1 \\ \beta_0 + \beta_1 \frac{R}{705} + \sigma & i = 2, \dots, 6 \end{cases} \quad (1)$$

Coefficients are given in Table 2 and the corresponding magnitude scaling models for each parameter are shown below. $S_{1,1}$ is an additive factor to $\ln(I_a)$; while $S_{1,i}$ for the other parameters are simple scalars. Note that these magnitude scaling models are for adjusting parameters from a 5.8 to a 7.6 magnitude. Linear interpolation can be used to obtain parameters for any size event between the two magnitudes.

$$S_{1,i} = \begin{cases} c_0 - c_1 \ln(R) & i = 1, 2, 3 \\ c_0 - c_1 R & i = 4, 6 \end{cases} \quad (2)$$

To calculate the value of $S_{2,i}$ for the i^{th} parameter at a given distance, we simply take the ratio of that parameter calculated for the two

different magnitudes, using our WUS model from Rezaeian and Der Kiureghian (2010). This ratio is then applied to the predicted value of that parameter from our Mineral model.

Table 2: Coefficients for scaling of model parameters

Param.	i	β_0	β_1	c_0	c_1
I_a	1	-0.164	-2.126	4.202	-0.534
D_{5-95}	2	-2.258	2.260	1.973	-0.121
t_{mid}	3	-2.869	2.894	1.886	-0.139
ω_{mid}	4	2.511	-2.517	0.756	-0.0006
ω'	5	-1.103	1.097	NA	NA
ζ	6	-0.110	0.129	1.761	-0.00004

5. COMPARISON WITH GMPE

There are no recordings for a magnitude 7.6 event in the CEUS, but we can compare our simulations to existing GMPEs for this region. Figure 8 shows the 0.2 s acceleration response versus distance for the physics-based simulation (using four different source models), and the stochastic simulation (using two different scaling models).

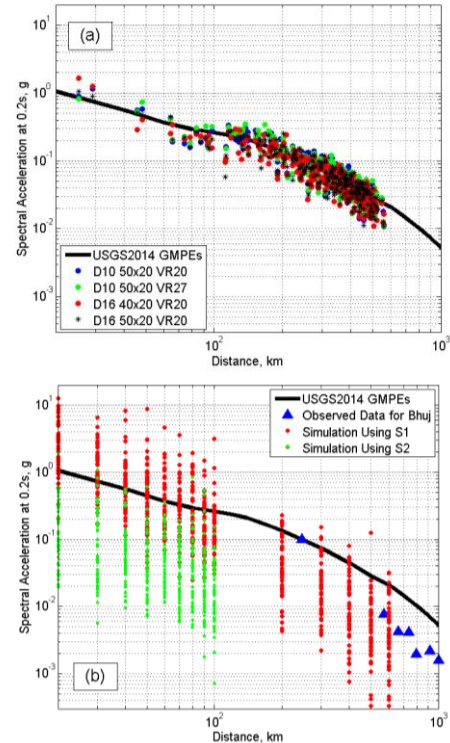


Figure 8: Acceleration response spectrum at 0.2 s for (a) physics-based simulations and (b) stochastic simulations of a M_w 7.6 event in the CEUS.

On each figure (8a and 8b), the weighted combination of GMPE medians in the CEUS, according to the USGS model by Petersen et al. (2014), is superimposed for reference. Note that there is a wide spread of GMPEs that is not shown here. Our simulations suggest a slightly faster fall-off with distance compared to the GMPE and a slightly smaller median for the stochastic model (as is also suggested by the data from Bhuj) than the GMPE shown in this figure. Also, note the lower ground motions at short distances if we were to use magnitude scaling based on WUS data (green dots in Figure 8b).

6. CONCLUSIONS

We used two simulation models, a deterministic physics-based approach and a site-based stochastic approach, to simulate ground motions for a large magnitude event in the CEUS. To do this, we used recordings from a moderate magnitude event in the CEUS, i.e., the 2011 M_w 5.8 Mineral earthquake, to establish our base regional models. Then, we used recordings from a large magnitude event in a similar tectonic setting, i.e., 2001 M_w 7.6 Bhuj, India, earthquake, to modify our parameters for a larger event in the CEUS. Both models show a good fit to data, but suggest a faster fall-off at large distances than existing GMPEs.

7. ACKNOWLEDGMENT

We gratefully acknowledge the receipt of the Bhuj records from the India Meteorological Department through Dr. Krishna Singh. This study is supported by the USGS Earthquake Hazards Program funding.

8. REFERENCES

Antolik, M., and D. S. Dreger (2003). Rupture process of the 26 January 2001 Mw 7.6 Bhuj, India, earthquake from teleseismic broadband data, *Bull. Seism. Soc. Am.* **93**: 1235-1248.

Atkinson, G. M. (2004). Empirical attenuation of ground-motion spectral amplitudes in southeastern Canada and the northeastern United States. *Bull. Seism. Soc. Am.* **94**: 1079-1095.

Boore, D. M. (2003). Simulation of ground motion using the stochastic method. *Pure Appl. Geophys.* **160**: 635–676.

Hartzell, S., M. Guatteri, P. Martin Mai, P.-C. Liu, and M. Fisk (2005). Calculation of broadband time-series of ground motion, part II: kinematic and dynamic modeling using theoretical Green's functions and comparison with the 1994 Northridge earthquake, *Bull. Seismol. Soc. Am.* **95**: 614-645.

Hartzell, S., and C. Mendoza (2011). Source and site response study of the 2008 Mount Carmel, Illinois, earthquake, *Bull. Seismol. Soc. Am.* **101**: 951-963

Petersen, M.D., Moschetti, M.P., Powers, P.M., Mueller, C.S., Haller, K.M., Frankel, A.D., Zeng, Y., Rezaeian, S., Harmsen, S.C., Boyd, O.S., Field, E., Chen, R., Rukstales, K.S., Luco, N., Wheeler, R.L., Williams, R.A., and Olsen, A.H., 2014, *Documentation for the 2014 Update of the United States National Seismic Hazard Maps*, U.S. Geological Survey Open-File Report 2014–1091, 242 p.

Rezaeian, S., and Der Kiureghian, A. (2010). Simulation of synthetic ground motions for specified earthquake and site characteristics. *Earthquake Engineering and Structural Dynamics*, **39**: 1155–1180.

Saikia, C. K. (1994). Modified frequency-wavenumber algorithm for regional seismograms using Filon's quadrature: Modelling of Lg waves in eastern North America, *Geophysical Journal International* **118**: 142-158.

Singh, S. K., B. K. Bansal, S. N. Bhattacharya, J. F. Pacheco, R. S. Dattatrayam, M. Ordaz, G. Suresh, Kamal, and S. E. Hough (2003). Estimation of ground motion for Bhuj (26 January 2001; Mw 7.6) and for future earthquakes in India, *Bull. Seism. Soc. Am.* **93**: 353-370.

Sun, X., S. Hartzell, and S. Rezaeian (2014). Ground motion simulation for the 23 August 2011, Mineral, Virginia earthquake using physics-based and stochastic broadband methods, *Bull. Seism. Soc. Am.*, in press.